CrossMark

ORIGINAL PAPER

Band Structure Simulations of the Structural, Electronic, Magnetic, and Half-Metallic Features of the $Ti_2CoAl_{1-x}Sn_x$ ($x = 0, 0.25, 0.50, 0.75, 1$) Heusler Alloys

F. Dahmane[1,2] · R. Khenata[2] · B. Doumi[3] · S. Bin Omran[4] · I. V. Kityk[5] · Sandeep[6] ·
A. Tadjer[7] · S. V. Syrotyuk[8] · D. P. Rai[9]

Abstract First-principles density functional theory (DFT) calculations with the generalized gradient approximation (GGA) have been performed to investigate electronic band structures and magnetic and half-metallic characteristic of $Ti_2CoAl_{1-x}Sn_x$ ($x = 0, 0.25, 0.50, 0.75, 1$). The optimized equilibrium lattice constants were found to be equal to 6.08 and 6.37 Å for Ti_2CoAl and Ti_2CoSn, respectively. These ternary Heusler compounds are found to be a complete half-metal with a total magnetic moment of 2 and 3 μ_B, respectively, which is in good compliance with the Slater–Pauling rule, $M_{total} = Z_{total} - 18$. The spin-polarized band structures and density of states (DOS) of the $Ti_2CoAl_{1-x}Sn_x$ (0.25, 0.50, and 0.75) Heusler alloys confirm that they are half-metal due to the presence of the energy gap in the minority spin. Consequently, $Ti_2CoAl_{1-x}Sn_x$ ($x = 0, 0.25, 0.50, 0.75, 1$) alloys are predicted to be a promising candidate for the practical applications in spintronic devices.

✉ F. Dahmane
fethallah05@gmail.com

R. Khenata
khenata_rabah@yahoo.fr

1 Département de SM, Institue des Sciences et des Technologies, Centre Universitaire de Tissemsilt, 38000 Tissemsilt, Algeria

2 Laboratoire de Physique Quantique de la Matière et de Modélisation Mathématique (LPQ3M), Université de Mascara, 29000 Mascara, Algeria

3 Faculty of Sciences, Department of Physics, Dr. Tahar Moulay University of Saida, 20000 Saida, Algeria

4 Department of Physics and Astronomy, College of Science, King Saud University, P.O. Box 2455, Riyadh 11451, Saudi Arabia

5 Faculty of the Electrical Engineering, Czestochowa University of Technology, Al. Armii Krajowej 17, 42-200 Czestochowa, Poland

6 Condensed Matter Theory Research Group, Department of Physics, Mizoram University, Aizawl 796004, India

7 Modelling and Simulation in Materials Science Laboratory, Physics Department, University of Sidi Bel-Abbes, 22000 Sidi Bel-Abbes, Algeria

8 Semiconductor Electronics Department, National University "Lviv Polytechnic", S. Bandera str. 12, Lviv 79013, Ukraine

9 Department of Physics, Pachhunga University College, Aizawl 796001, India

1 Introduction

Heusler alloys with the general chemical formula X_2YZ, where the X and Y atoms are transition metals and Z is a nonmagnetic metal or a nonmetallic element, have been attracting considerable interest due to their unique transport and magnetic properties [1], and they are the objects of great attention of researchers. In addition, they also serve as a source of new ideas and concepts on the formation of the electronic structure of magnets [2] and other spin-polarized compounds. Heusler alloys are known to be the essential ingredient for spintronic devices because some of them have been predicted to demonstrate half-metallicity, which maximizes the spin injection rate from ferromagnetic

to semiconducting materials [3]. Half-metallic ferromagnets (HMFs) have shown great potential in spintronic devices since their introduction by de Groot and colleagues in the early 1980s [4]. Ideal half-metals (HMs) exhibit no energy bandgap for one spin channel, while indicating semiconductor behaviour for the other spin channels at the Fermi level. Due to the gap for one spin direction, the density of states at the Fermi level has 100 % theoretical spin polarization. The NiMnSn with the C_{1b} structure is the first predicted HM ferromagnet [5]. In recent years, half-metallic ferromagnetism has been investigated for X_2MnGe (X = Sc, Fe, Ni) [6], Ti_2ZAl (Z = Co, Fe, Mn) [7], Co_2CrX (X = Al, Ga, In) [8], Co_2MnZ (Z = Al, Ge, Si, Ga) [9], and Fe_2XAl (X = Cr, Mn, Ni) [10].

A few studies have been performed for the Ti_2-based HM Heusler alloys. Feng et al. [11] used first-principles calculations to show that the full-Heusler compound Ti_2NiAl with a Hg_2CuTi-type structure is a new HM ferromagnet. Kervan et al. studied the electronic and the magnetic properties of the full-Heusler Ti_2CoGa [12], Ti_2CoAl [13], Ti_2FeSi [14], and Ti_2CoB [15] compounds. They predicted that all these compounds were HM ferrimagnets with a total magnetic moment of 2 μ_B and that a complete spin polarization (100 %) exists around the Fermi level at the equilibrium lattice constant. Recently, Zheng and Jin [16] explored the half-metallicity of full-Heusler Ti_2YAl (Y = V, Cr, Mn, Fe, Co, Ni, Cu, and Zn) alloys with the $CuHg_2Ti$-type structure, and they showed that the Ti_2MnAl alloy was a HM antiferromagnet, the Ti_2YAl (Y = Fe, Co, and Ni) alloys were HM ferrimagnets, and the Ti_2YAl (Y = V, Cr, Cu, and Zn) alloys were conventional ferromagnets [17]. In this paper, we present a study on the $Ti_2CoAl_{1-x}Sn_x$ (x = 0, 0.25, 0.50, 0.75, 1) Heusler alloys. In these alloys, up to now, no reports on the half-metallicity have been reported for x = 0.25, x = 0.50, and x = 0.75. Therefore, it is necessary to systematically study the structural, electronic, and magnetic properties and the half-metallic behaviour of the $Ti_2CoAl_{1-x}Sn_x$ (x = 0, 0.25, 0.50, 0.75, 1) alloys by the density functional calculations. This paper is structured as follows, where a brief description of the theoretical method and the different parameters used in our calculations is presented in Section 2. Through Section 3, we discuss the ground-state properties of the considered ternary compounds and their quaternary as well as their electronic band structures and magnetic properties. Finally, the results are summarized in Section 4.

2 Computational Details

The calculations of the present study are performed within a framework of the density functional theory (DFT) [18, 19].

We have utilized the full-potential linearized augmented plane wave (FP-LAPW) method as implemented in the WIEN2k code [20], which is one of the most accurate methods of simulating and calculating the ground-state properties of crystalline materials [21]. The exchange correlation term has been considered within the generalized gradient approximation (GGA) [22] to study the electronic structure and magnetic properties of $Ti_2CoAl_{1-x}Sn_x$ (x = 0, 0.25, 0.50, 0.75, 1). The basic functions are expanded into spherical harmonic functions and Fourier series inside the muffin-tin sphere and in the interstitial regions, respectively. The muffin-tin sphere radii were 2.37 a.u. for Ti and Co and 2.23 a.u. for Al in Ti_2CoAl and were 2.46 a.u. for Ti and Co and 2.31 for Sn in Ti_2CoSn, respectively. The maximum value of the angular momentum (l_{max} = 10) is taken for the wave function expansion inside the muffin-tin spheres. The convergence of the basis set was controlled by a cutoff parameter, $R_{MT} \cdot K_{max}$ = 7, where R_{MT} is the smallest muffin-tin sphere radius and K_{max} is the largest reciprocal lattice vector used in the plane wave expansion within the interstitial region. The cutoff energy, which defines the separation of the valence and core states, was chosen as 6 Ry. We select the charge convergence as $0.0001e$ during the self-consistency cycles. The magnitude of the largest vector in the charge density Fourier expansion was G_{max} = 14 (a.u.)$^{-1}$. A mesh of 64 special Brillouin zone (BZ) **k**-points was used in the irreducible wedge of the BZ. The total energy dependence on the cell volume is fitted to the Murnaghan equation of state [23] to determine the ground-state properties, as shown in (1)

$$E = E_0(V) + \frac{BV}{B'(B'-1)} \left[B(1 - \frac{V0}{V}) + \left(\frac{V0}{V}\right)^{B'} - 1 \right]$$
(1)

where E_0 is the minimum energy at T = 0 K, B is the bulk modulus, B' is the bulk modulus derivative, and V_0 is the equilibrium volume. In order to simulate the $Ti_2CoAl_{1-x}Sn_x$ (x = 0.25, 0.50, 0.75) quaternary alloy, we have used a supercell with 16 atoms. For x = 0.25, we substituted one atom of Al by Sn; for x = 050, we substituted two atoms of Al by two atoms of Sn; and for x = 0.75, we substituted three atoms of Al by three atoms of Sn. The crystal structure of $Ti_2CoAl_{1-x}Sn_x$ (x = 0, 0.25, 0.50, 0.75, 1) is shown in Fig. 1.

3 Results and Discussion

In this section, we present the results of the geometrical structure optimization for the $Ti_2CoAl_{1-x}Sn_x$ (x = 0, 0.25, 0.50, 0.75, 1) Heusler alloys in addition to the lattice
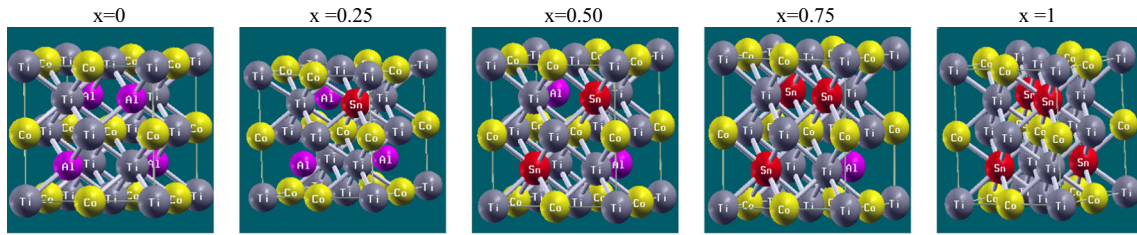
Fig. 1 Crystal structure of the $Ti_2CoAl_{1-x}Sn_x$ crystalline alloys ($x = 0, 0.25, 0.50, 0.75, 1$)

parameters and bulk modulus. The variation of the total energy with the volume is fitted to the Murnaghan equation of state [23] to obtain the equilibrium lattice constant and bulk modulus. The X_2YZ Heusler compounds, which crystallize in the cubic L_{21} structure, have two types: the Cu_2MnAl and Hg_2CuTi structures. The two structures consist of four inter-penetrating Fcc sublattices, which have four unique crystallites. In the case of the Cu_2AlMn-type L_{21} structure, the sequence of the atoms occupying the four sites of the unit cell is X–Y–X–Z, where the X atoms occupy positions A (0, 0, 0) and C (1/2, 1/2, 1/2) and the Y and Z atoms are located at B (1/4, 1/4, 1/4) and D (3/4, 3/4, 3/4), respectively. While for the Hg_2CuTi-type L_{21} structure, the Y and the second X exchange sites and the sequence of the atoms is X–X–Y–Z, where the X atoms occupy the A (0, 0, 0) and B (1/4, 1/4, 1/4) sites, the Y atom occupies the C (1/2, 1/2, 1/2) site, and the Z atom occupies the D (3/4, 3/4, 3/4) site, respectively. The equilibrium lattice constants, bulk modulus, and these first derivatives are presented in Table 1. The optimized lattice constants for the Ti_2CoAl and Ti_2CoSn alloys are 6.08 and 6.37 Å, respectively, and they are in fairly good accordance with the previous theoretical calculations of 6.14 Å [13, 16] and 6.36 Å [17]. To the best knowledge of the author, there are no comparable studies about $Ti_2CoAl_{1-x}Sn_x$ ($x = 0.25, 0.50,$ and 0.75) in

the literature. Hence, we estimated the lattice parameters by Vegard's law in Eq. (2)

$$Ti_2CoAl_{1-0.25}Sn_{0.25} : a(\text{Å}) = 6.08 \times (1 - 0.25)$$
$$+ 6.37 \times 0.25 = 6.1525 \text{ Å}$$
$$Ti_2CoAl_{1-0.50}Sn_{0.5} : a(\text{Å}) = 6.08 \times (1 - 0.5)$$
$$+ 6.37 \times 0.5 = 6.225 \text{ Å}$$
$$Ti_2CoAl_{1-0.75}Sn_{0.75} : a(\text{Å}) = 6.08 \times (1 - 0.75)$$
$$+ 6.37 \times 0.75 = 6.2975 \text{ Å}$$
$$(2)$$

For the Ti_2CoAl and Ti_2CoSn inverse Heusler alloys, the spin-polarized band structure and the total density of states (DOS) are depicted in Figs. 2 and 3, respectively. It is clear from Fig. 2 that the majority-spin oriented bands are metallic while the minority-spin oriented band shows a semiconducting gap around the Fermi level. This energy gap in the minority-spin band leads to almost 100 % spin polarization at the Fermi level, and this energy gap can be calculated using the energies of the highest occupied band at the Γ point and the lowest unoccupied band at the X point.

Figure 3 shows a minority-spin channel where the total DOS in the region of the Fermi level is mainly due to the presence of the d electrons of the Ti(1), Ti(2), and Co transition metals. One can see the presence of the majority-spin states at the Fermi level and a wide bandgap in the minority-spin state confirming the HM characteristic of Ti_2CoAl and Ti_2CoSn. Within the -5 to -1 eV energy range, the s electrons of Al are contributed prevailingly. The minority-spin bandgap is an essential factor in the HM materials, and the cause of the HM bandgap is discussed as follows. The HM bandgaps usually take place from three aspects [17]: the covalent bandgap which exists in the half-Heusler alloy with the C_{1b} structure, the d–d bandgap that is originated from the HM bandgap in the full-Heusler alloys with the $AlCu_2Mn$ structure, and finally, the charge transfer bandgap [17] which is usually observed in CrO_2 and double perovskites [17]. For the Ti_2CoAl and Ti_2CoSn crystalline alloys with the Hg_2CuTi-type structure, the Ti atoms occupy two sublattices with different coordination environments. In addition, the Ti_2CoAl and Ti_2CoSn alloys with the

Table 1 The calculated lattice constant (a, Å), bulk modulus (B, GPa), first derivative (B′), and HM bandgap for the $Ti_2CoAl_{1-x}Sn_x$ (x = 0, 0.25, 0.50, 0.75, 1) alloys

Compound	a (Å)	B (GPa)	$B′$	E_g (eV)
Ti_2CoAl	6.08	145.3581	4.5971	0.63
	6.14 [13]	134.134 [13]	3.929 [13]	0.49 [13]
	6.142 [16]			0.68 [24]
Ti_2CoSn	6.37	143.6663	7.5878	0.84
	6.36 [17]	127.37 [17]	4.43 [17]	0.8 [17]
$Ti_2CoAl_{0.75}Sn_{0.25}$	6.24	115.2747	3.1832	0.53
$Ti_2CoAl_{0.50}Sn_{0.50}$	6.27	242.7048	11.1280	0.5605
$Ti_2CoAl_{0.25}Sn_{0.75}$	6.34	144.1758	4.6305	0.56324
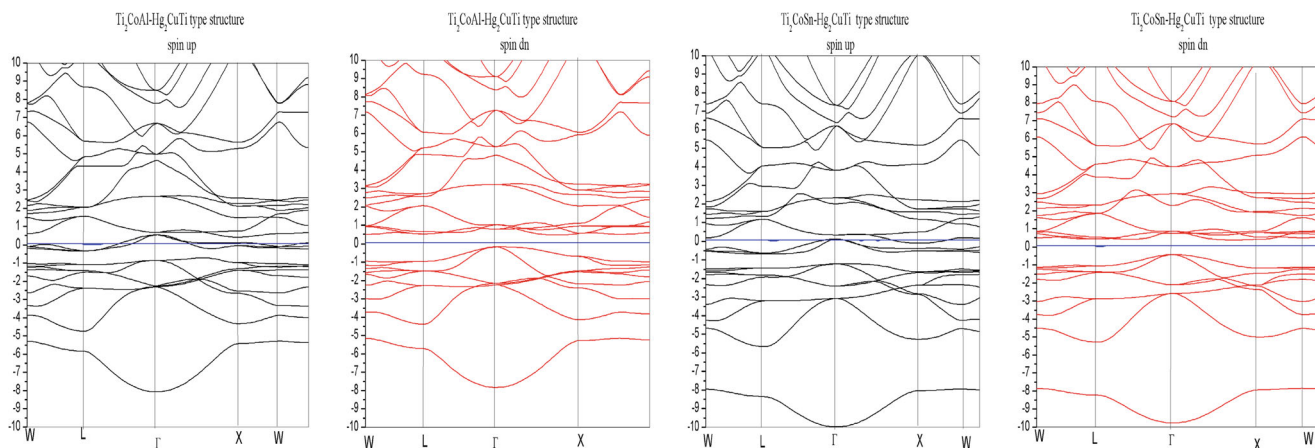
Fig. 2 The spin-polarized band structure of Ti$_2$CoAl and Ti$_2$CoSn

Hg$_2$CuTi-type structure have a space group which is similar to that one of the half-Heusler alloys, but with an additional occupied site. Therefore, investigation of the origin of the bandgap in the Hg$_2$CuTi-type structure of the Ti$_2$CoAl and Ti$_2$CoSn alloys is important [25].

The origin of the bandgap in Ti$_2$FeSn, for example, has been discussed by Ahmadian [25]: Ti(1) and Ti(2) atoms have tetrahedral T$_d$ symmetry, and the d orbital of these atoms is divided into doubly and triply degenerated orbital, i.e., e_g (d_{x2-y2}, d_{z2}) and t_{2g} (d_{xy}, d_{yz}, d_{zx}) orbitals. A strong hybridization exists between the t_{2g} (e_g) states of Ti(1) and Ti(2), leading to bonding and antibonding of the e_g and the t_{2g} states. Similarly, the Fe atom has a T$_d$ symmetry, and the d orbitals split into doubly degenerated e_g (d_{x2-y2}, d_{z2}) and triply degenerated t_{2g} (d_{xy}, d_{yz}, d_{zx}) states. The e_g and the t_{2g} states of the Ti(1)–Ti(2) coupling are further hybridized with the e_g and the t_{2g} states of Fe, which results in the bonding (e_g, t_{2g}) and antibonding (e_g, t_{2g}) states. At the same time, the Fermi level is located in the gap between

the bonding t_{2g} and the antibonding t_{2g} states. Within the group theory symmetry analysis, the antibonding states of the Ti(1)–Ti(2) coupling cannot be hybridized to the e_g and the t_{2g} states of Fe. Therefore, the d–d hybridization between transition metals can participate in the formation of the minority bandgap [25].

The spin-polarized band structure and the total DOS for Ti$_2$CoAl$_{1-x}$Sn$_x$ (x = 0.25, 0.50, and 0.75) are presented in Figs. 4 and 5, and we can observe that E_F cuts all the way through the bands in the majority-spin channel, which is the spin-up case, while the energy gap of Ti$_2$CoAl$_{1-x}$Sn$_x$ (x = 0.25, 0.50, and 0.75) resides in the minority-spin channel (spin-down). This means that the majority-spin states have a metallic character, while the minority-spin band contains an energy gap at the Fermi level (E_F), which is a semiconducting one. This suggests that Ti$_2$CoAl$_{1-x}$Sn$_x$ (x = 0.25, 0.50, and 0.75) are half-metals and electrons at the Fermi level are 100 % spin-polarized. It is necessary to emphasize the substantial anisotropy of the electron bands
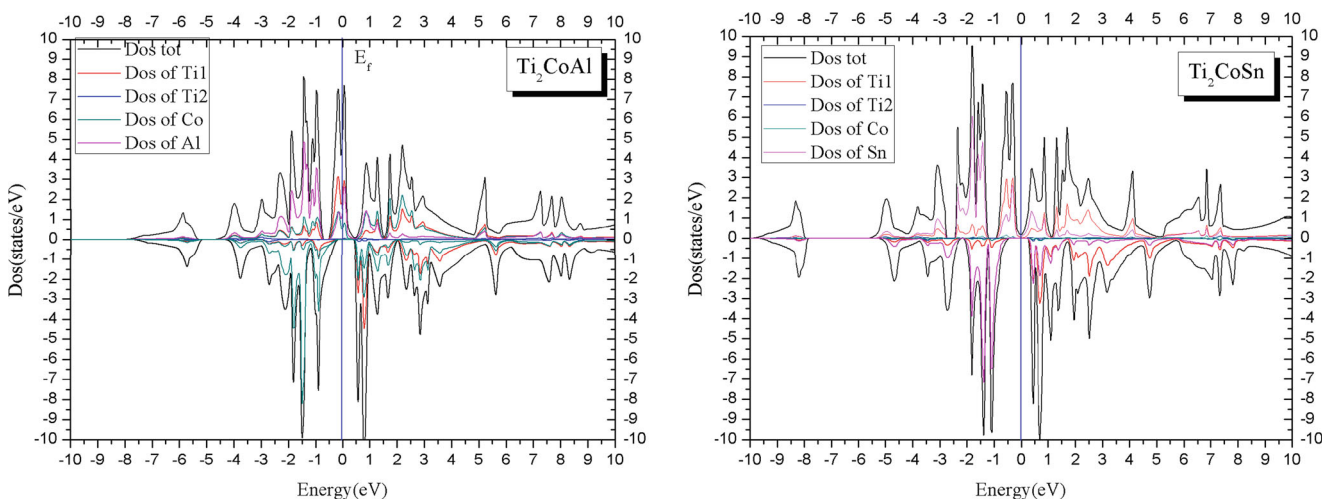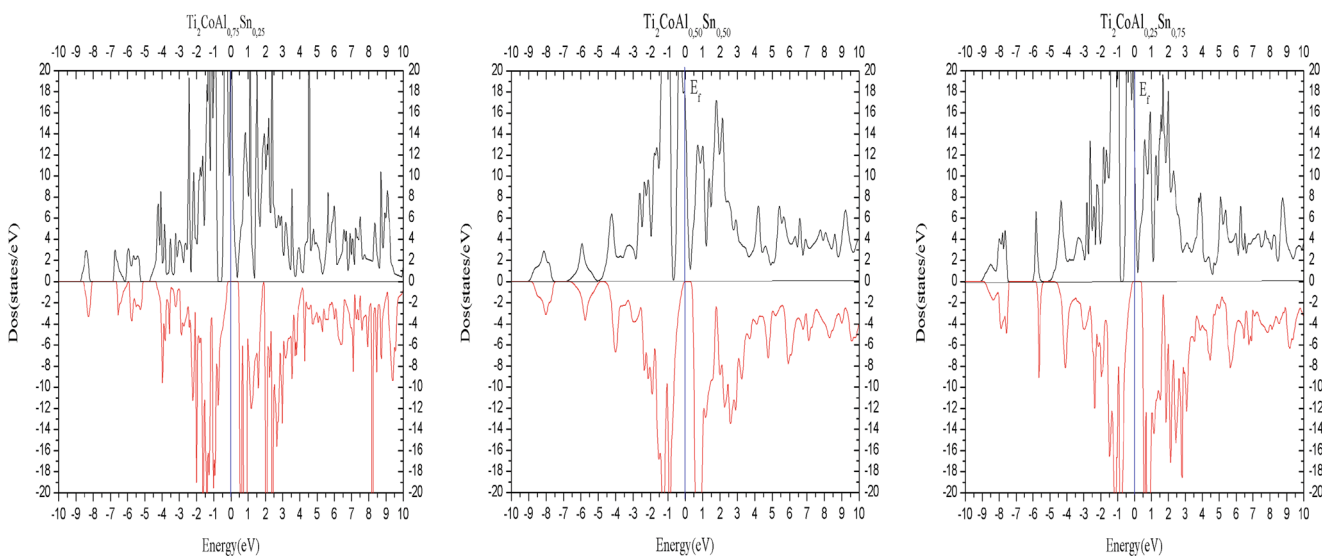

Fig. 3 DOS of Ti$_2$CoAl and Ti$_2$CoSn in the Hg$_2$CuTi-type structures
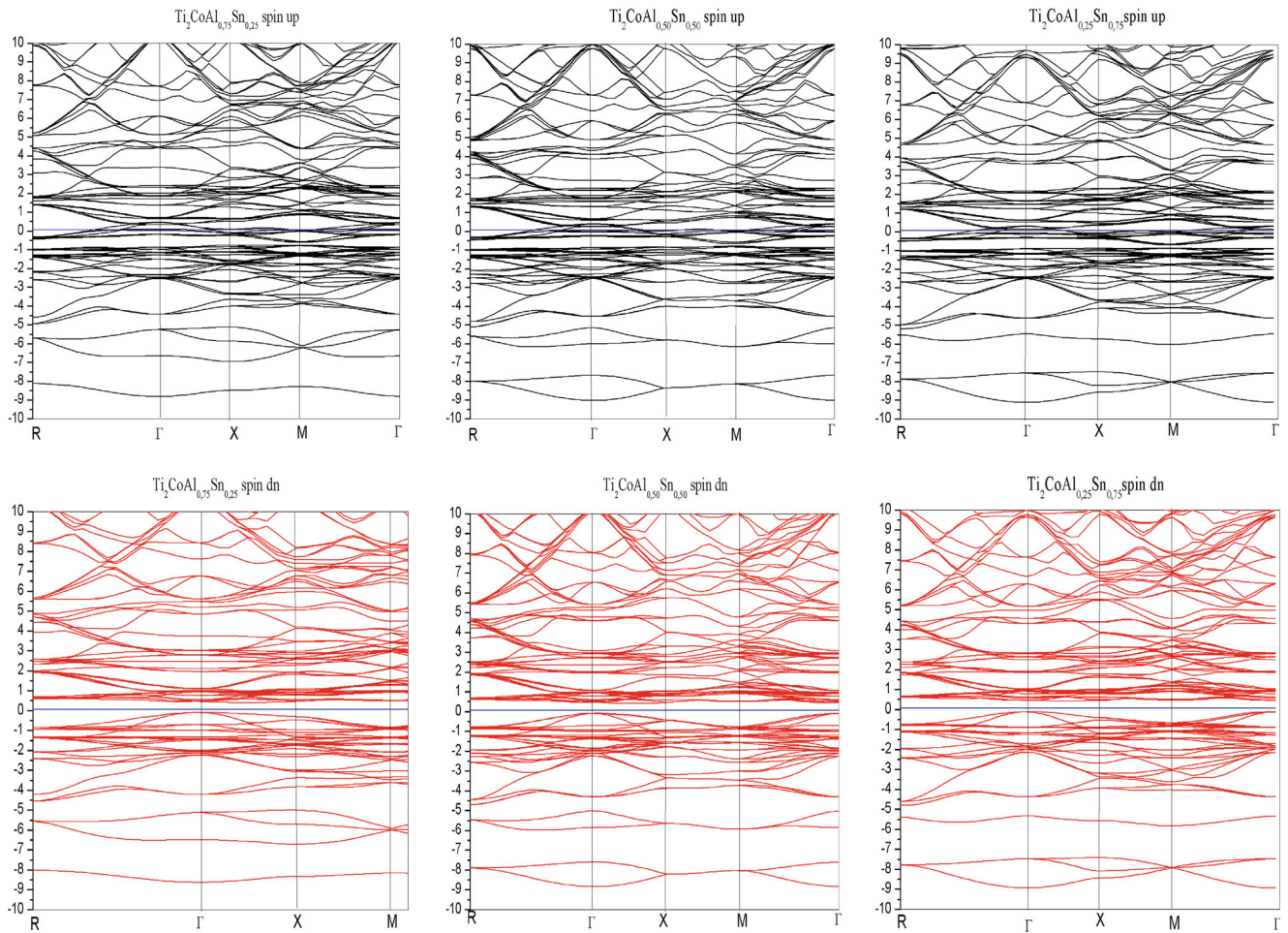
Fig. 4 The spin-polarized band structure of $Ti_2CoAl_{1-x}Sn_x$ ($x = 0.25, 0.50, 0.75$)

Fig. 5 DOS of $Ti_2CoAl_{1-x}Sn_x$ ($x = 0.25, 0.50, 0.75$)

Table 2 The total and partial magnetic moments of $Ti_2CoAl_{1-x}Sn_x$ ($x = 0, 0.25, 0.50, 0.75, 1$)

Compound	$M_{Ti(1)}$	$M_{Ti(2)}$	M_{Co}	M_{Al}	M_{Sn}	$M_{interstitial}$	M_{total}
Ti_2CoAl	1.14807	0.65137	−0.29248	−0.00109	–	0.49423	2.00
	1.101 [16]	0.598 [16]	−0.188 [16]	0.014 [16]	–		2.00 [16]
							2.00 [13]
Ti_2CoSn	1.41715	0.73736	0.36232	–	−0.00594	0.48920	3.00
	1.27 [17]	0.65 [17]	0.36 [17]	–	−0.003 [17]	0.72 [17]	3.00 [17]
$Ti_2CoAl_{0.75}Sn_{0.25}$							8.99978
$Ti_2CoAl_{0.50}Sn_{0.50}$							9.99942
$Ti_2CoAl_{0.25}Sn_{0.75}$							10.99964

for two directions: R–X–M and G–X. This factor may be indicated on different hole mobilities in these directions, particularly in the R–X–M BZ direction as there are more delocalized band carriers and in the G–X direction as there are more localized states.

Slater and Pauling discovered that the magnetic moment (m) for the 3d elements and their binary alloys can be estimated on the basis of the average valence electron number (N_V) per atom [26, 27]. The materials are divided into two areas depending on the magnetic moment near N_V: The first area of the Slater–Pauling curve is the area of low-valence electron concentrations ($N_V \leq 8$) and of localized magnetism. The second area is the area of high-valence electron concentrations ($N_V \geq 8$) and of itinerant magnetism where the magnetic moment is in multiples of Bohr magnetons (μ_B) given by $m = N_V − 2n \downarrow$, where $2n \downarrow$ denotes the number of electrons in the minority-spin states. The half-metallic materials obey the Slater–Pauling rule [26, 27]: $m_{HMF} \approx N_V − 6$, where m_{HMF} is the mean magnetic moment per atom. In the case of the compounds having four atoms per unit cell, one has to subtract 24 (6 multiplied by the number of atoms) from the accumulated number of valence electrons in the unit cell N_V to find the spin magnetic moment per unit cell: $m_{HMF} = N_V − 24$.

Recent research reveals that many Ti_2-based full-Heusler alloys with the Hg_2CuTi-type structure can also belong to the family of half-metallic material, and the total magnetic moments of these alloys follow the $M_{total} = Z_{total} − 18$ rule instead of the $M_{total} = Z_{total} − 24$ rule [13]. The Ti_2CoAl alloy has 20 valence electrons per unit cell ($Z_{total} = 20$), and therefore, the spin magnetic moment is $20 − 18 = 2 \mu_B$ for each unit cell. The Ti_2CoSn alloy has 21 valence electrons per unit cell, so the spin magnetic moment is $21 − 18 = 3 \mu_B$.

The calculated total magnetic moment of the Ti_2CoAl compound is 2 μ_B (as shown in Table 2), while the atomic magnetic moments are 1.14 μ_B for Ti(1), 0.65137 μ_B for Ti(2), −0.29248 μ_B for Co, 0.00109 μ_B for Al, and 0.49423 μ_B for Sn, respectively, for the interstitial moment. For Ti_2CoSn, the total magnetic moment is 3 μ_B with the atomic magnetic moments: 1.41715, 0.73736, 0.36232,

−0.00594, and 0.48920 μ_B for Ti(1), Ti(2), Co, Sn, and interstitial moments, respectively. The atom magnetic moments for Ti_2CoAl in the present study are in good agreement with the results reported by Zheng et al. [16] and Bayar et al. [13]. The calculated integer magnetic moment of the Ti_2CoAl and Ti_2CoSn compounds indicates the stability of half-metallic behaviour. It is seen that the total magnetic moment per unit cell is increased as a function of x concentration (2 μ_B, 9 μ_B/16 atoms, 10 μ_B/16 atoms, 11 μ_B/16 atoms, and 3 μ_B, for $x = 0, 0.25, 0.50, 0.75,$ and 1, respectively), for $Ti_2CoAl_{1-x}Sn_x$ ($x = 0, 0.25, 0.50, 0.75, 1$). It can be seen from Table 2 that the different local magnetic moments for the two Ti atoms in the Ti_2CoAl and Ti_2CoSn alloys with the $CuHg_2Ti$-type structure originated from different atomic environments, i.e., the Ti(1) atom has four nearest Ti(2) atoms and four nearest Al (Sn) atoms as well as six second-nearest Co atoms, while the Ti(2) atom has four nearest Ti(1) atoms and four nearest Co atoms as well as six second-nearest Al (Sn) atoms.

The presented results may be helpful for the analysis of magnetic spin polarization for other half-metallicity in Heusler alloys such as Zr_2VZ (Z = Al, Ga, In) [28], Ti_2YPb (Y = Co, Fe) [29], and Mn_2ZrSi and Mn_2ZrGe [30]. All these compounds are characterized by an enhanced number of defect states which may change experimentally observed magnitudes of magnetization.

4 Conclusions

For the $Ti_2CoAl_{1-x}Sn_x$ ($x = 0, 0.25, 0.50, 0.75, 1$) Heusler alloys, the electronic structure and magnetic properties have been calculated using the first-principles FP-LAPW method. The spin-polarized calculations showed that the Ti_2CoAl and Ti_2CoSn Heusler compounds are a half-metallic with a magnetic moment of 2 and 3 μ_B, respectively. $Ti_2CoAl_{1-x}Sn_x$ ($x = 0, 0.25, 0.50, 0.75, 1$) indicates that the quaternary Heusler alloys have a perfect half-metallic character with semiconducting minority-spin

band structure and 100 % polarization. Consequently, $Ti_2CoAl_{1-x}Sn_x$ (x = 0, 0.25, 0.50, 0.75, 1) is predicted to be a good promising candidate to explore the half-metallic ferromagnetism for the practical applications of spintronic devices. The calculations have shown a substantial anisotropy of electron bands for two BZ directions: R–X–M and G–X. This factor may be indicated on different hole mobilities in these directions, particularly in the R–X–M direction where there are more delocalized band carriers and in the G–X direction where there are more localized states. This may be used for the creation of different spintronic devices.

References

1. Fukatani, N., Fujita, H., Miyawaki, T., Ueda, K., Asano, H.: J. Kor. Phys. Soc. **63**(3), 711–715 (2013)
2. Shreder, E.I., Svyazhin, A.D., Fomina, K.A.: Phys. Met. Metallogr. **113**, 146 (2012)
3. Quang, T.V., Lee, J.I., Kim, M.: J. Kor. Phys. Soc. **62**(12), 2184–2187 (2013)
4. de Groot, R.A., Mueller, F.M., van Engen, G.P., Buschow, K.H.J.: Phys. Rev. Lett. **50**, 2024 (1983)
5. Wei, X.-P., Chu, Y.-D., Sun, X.-W., Deng, J.-B.: Eur. Phys. J. B **86**, 450 (2013)
6. Dahmane, F., Mesri, D., Doumi, B., Tadjer, A., Abbar, B., Yakoubi, A., Boutaleb, M., Aourag, H.: J. Supercond. Nov. Magn. doi:10.1007/s10948-015-2994-9
7. Dahmane, F., Benalia, S., Djoudi, L., Tadjer, A., Khenata, R., Doumi, B., Aourag, H.: J. Supercond. Nov. Magn. doi:10.1007/s10948-015-3109-3
8. Dahmane, F., Mesri, D., Tadjer, A., Khenata, R., Benalia, S., Djoud, L., Doumi, B., Boumia, L., Aourag, H.: Mod. Phys. Lett. B **30**, 1550265 (2016)
9. Dahmane, F., Doumi, B., Mogulkoc, Y., Tadjer, A., Prakash, D., Verma, K.D., Varshney, D., Gheboul, M.A., Bin Omran, S., Khenata, R.: J. Supercond. Nov. Magn. doi:10.1007/s10948-015-3357-2
10. Dahmane, F., Mogulkoc, Y., Doumi, B., Tadjer, A., Khenata, R., Bin Omran, S., Rai, D.P., Murtaza, G., Varshney, D.: J. Magn. Magn. Mater. **407**, 167 (2016)
11. Feng, L., Tang, C., Wang, S., He, W.: J. Alloy. Comp. **509**, 5187 (2011)
12. Kervan, N., Kervan, S.: J. Magn. Magn. Mater. **324**, 645 (2012)
13. Bayar, E., Kervan, N., Kervan, S.-U.: J. Magn. Magn. Mater. **323**, 2945 (2011)
14. Kervan, N., Kervan, S.: J. Phys. Chem. Solids **72**, 1358 (2011)
15. Kervan, N., Kervan, S.: Solid State. Commun. **151**, 1162 (2011)
16. Zheng, N., Jin, Y.: J. Magn. Magn. Mater. **324**, 3099 (2012)
17. Ahmadian, F.: J. Alloys Compd. **576**, 279 (2013)
18. Hohenberg, P., Kohn, W.: Phys. Rev. B **136**, 864 (1964)
19. Kohn, W., Sham, L.J.: Phys. Rev. A **140**, 1133 (1965)
20. Blaha, P., Schwarz, K., Madsen, G.K.H., Kvasnicka, D., Luitz, J.: WIEN2k, an Augmented Plane Wave Plus Local Orbitals Program for Calculating Crystal Properties. Vienna University of Technology, Vienna (2001)
21. Wong, K.M., Alay-e-Abbas, S.M., Fang, Y., Shaukat, A., Lei, Y.: J. Appl. Phys. **114**, 034901 (2013)
22. Perdew, J.P., Burke, K., Ernzerhof, M.: Phys. Rev. Lett. **77**, 3865 (1996)
23. Murnaghan, F.D.: Proc. Natl. Acad. Sci. USA **30**, 5390 (1944)
24. Wei, X.P., Deng, J.B., Mao, G.Y., Chu, S.B., Hu, X.-R.: Intermetallics **29**, 86 (2012)
25. Ahmadian, F.: J. Kor. Phys. Soci. **64**, 277 (2014)
26. Slater, J.C.: Phys. Rev. **49**, 537 (1936)
27. Pauling, L.: Phys. Rev. **54**, 899 (1938)
28. Gao, Y.C., Wang, X.T., Rozale, H., Lu, J.W.: J. Kor. Phys. Soc. **67**, 881 (2015)
29. Hussain, M.K., Gao, G.Y., Yao, K.-L.: Int. J. Mod. Phys. B **29**, 1550175 (2015)
30. Abada, A., Amara, K., Hiadsi, S., Amrani, B.: J. Magn. Magn. Mater **388**, 59 (2015)